SOCIETY FOR EXPERIMENTAL BIOLOGY

Journal of Experimental Botany, Vol. 74, No. 9 pp. 2860–2874, 2023
https://doi.org/10.1093/jxb/erad011 Advance Access Publication 12 January 2023

RESEARCH PAPER

The impact of growth at elevated [CO_2] on stomatal anatomy and behavior differs between wheat species and cultivars

Shellie Wall[1], James Cockram[2], Silvere Vialet-Chabrand[1,†], Jeroen Van Rie[3], Alexander Gallé[3] and Tracy Lawson[1,*]

[1] School of Life Sciences, University of Essex, Colchester CO4 3SQ, UK
[2] NIAB, 93 Lawrence Weaver Road, Cambridge CB3 0LE, UK
[3] BASF Belgium Coordination Center CommV-Innovation Center Gent, Technologiepark-Zwijnaarde 101, 9052 Gent, Belgium
[†] Present address: Horticulture and Product Physiology; WUR; Droevendaalsesteeg 1, 6708PB, Wageningen, The Netherlands.

* Corresponding author: tlawson@essex.ac.uk

Received 1 September 2022; Editorial decision 5 January 2023; Accepted 11 January 2023

Editor: John Lunn, MPI of Molecular Plant Physiology, Germany

Abstract

The ability of plants to respond to changes in the environment is crucial to their survival and reproductive success. The impact of increasing the atmospheric CO_2 concentration (a[CO_2]), mediated by behavioral and developmental responses of stomata, on crop performance remains a concern under all climate change scenarios, with potential impacts on future food security. To identify possible beneficial traits that could be exploited for future breeding, phenotypic variation in morphological traits including stomatal size and density, as well as physiological responses and, critically, the effect of growth [CO_2] on these traits, was assessed in six wheat relative accessions (including *Aegilops tauschii*, *Triticum turgidum* ssp. *Dicoccoides*, and *T. turgidum* ssp. *dicoccon*) and five elite bread wheat *T. aestivum* cultivars. Exploiting a range of different species and ploidy, we identified key differences in photosynthetic capacity between elite hexaploid wheat and wheat relatives. We also report differences in the speed of stomatal responses which were found to be faster in wheat relatives than in elite cultivars, a trait that could be useful for enhanced photosynthetic carbon gain and water use efficiency. Furthermore, these traits do not all appear to be influenced by elevated [CO_2], and determining the underlying genetics will be critical for future breeding programmes.

Keywords: Bread wheat, net CO_2 assimilation rate (*A*), stomatal density, stomatal conductance (g_s), *Triticum aestivum* L., wheat relatives (*Aegilops tauschii*, *Triticum turgidum* ssp. *dicoccoides*, and *Triticum turgidum* ssp. *dicoccon*).

Introduction

Prior to the industrial revolution, the atmospheric CO_2 concentration (a[CO_2]) was maintained at a value close to 280 ppm for ~1000 preceding years (Tans and Keeling, 2016). Subsequently, anthropogenic CO_2 emissions, primarily through the burning of fossil fuels, have increased the present day atmospheric CO_2 concentration to 419 ppm (NOAA, 2022). With the current increases in CO_2 emissions associated with modern day activities, the Intergovernmental Panel on Climate Change projections include scenarios of [CO_2] doubling from current levels by the end of the century (IPCC, 2021), which to date has resulted in a rise in global temperature (of ~1.1 °C, World Meteorological Organization, 2022) and is

predicted to rise with further increases in [CO_2] (Stockwell *et al.*, 2021). Elevated [CO_2] generally increases leaf photosynthetic rates in a range of C_3 crops from potatoes (Lawson *et al.*, 2001) to soybean (Rogers *et al.*, 2004), through increased substrate for Rubisco (the enzyme involved in the first major step of carbon fixation) and the suppression of photorespiration. A recent review of 18 C_3 crops grown using free-air CO_2 enrichment (FACE) technology with elevated CO_2 of 200 ppm above ambient [CO_2] reported that most species exhibited increased yields by ~18% (Ainsworth and Long, 2021). However, the same study also highlighted that yield increases were not consistent across species or cultivars, and yield benefits with elevated [CO_2] were correlated with sink strength (Ainsworth and Long, 2021).

As stomatal conductance (g_s) regulates gas exchange between the leaf interior and the external environment, stomatal responses to changing climatic conditions are critical in determining CO_2 supply for photosynthesis (A) and water loss through transpiration (Lawson *et al.*, 1998; Morison *et al.*, 2008). Transpirational water loss also plays a key role in nutrient uptake from the plant roots as well as evaporative cooling of the leaf tissue and the maintenance of optimal leaf temperatures for photosynthesis (Raven, 1977, 2002; Hetherington and Woodward, 2003; Peterson *et al.*, 2010; McAusland *et al.*, 2016; Murray *et al.*, 2016; Lawson and Vialet-Chabrand, 2019). Therefore, stomatal dynamics will have a pivotal role in determining C_3 crop productivity in future climates (Lawson *et al.*, 2010, 2012).

g_s is determined by anatomical features as well as functional aspects of the guard cells, both of which are influenced by growth [CO_2] (and temperature) (Woodward, 1987; Matthews and Lawson, 2019; Stevens *et al.*, 2021). Both stomatal anatomy and behavior are modified by elevated [CO_2], with most species responding by decreasing stomatal density (Woodward, 1987; Poole *et al.*, 1996) and reducing aperture (see review by Stevens *et al.*, 2021). Reducing stomatal aperture under elevated [CO_2] greatly increases intrinsic water use efficiency (WUEi; A/g_s) with potential benefits for plant growth (Leakey *et al.*, 2009; Sreeharsha *et al.*, 2015). On the other hand, reductions in g_s can negatively impact on photosynthesis through diffusional constraints, as well increases in leaf temperature (Matthews and Lawson, 2019).

The number and size of stomata on the leaf determine the maximum potential stomatal conductance (g_{smax}; Lawson and Morison 2004; Lawson *et al.*, 2010; McElwain *et al.*, 2016), whilst pore aperture/behavior regulates the short-time scale dynamics of g_s and gas exchange (Dow *et al.*, 2014; Takahashi *et al.*, 2015). The majority of studies that have explored variation in g_s or the influence of growth conditions on anatomy and function have examined steady-state conditions (Schlüter *et al.*, 2003; Doheny-Adams *et al.*, 2012; Tanaka *et al.*, 2013); however, recent studies have illustrated the significant impact of dynamic g_s responses on A (Sakoda *et al.*, 2020, 2022; Vialet-Chabrand and Lawson, 2020) and WUEi (Papanatsiou *et al.*, 2019; Acevedo-Siaca *et al.*, 2021; Pignon *et al.*, 2021). Generally, slow stomatal opening limits the CO_2 assimilation rate, reducing the speed of photosynthetic induction (Long *et al.*, 2022), whilst slow closure erodes WUEi (Lawson and Blatt, 2014; McAusland *et al.*, 2016; Qu *et al.*, 2016, 2020; Lawson and Vialet-Chabrand, 2019). The rapidity of stomatal responses to changing climatic conditions is also critically important for maintaining optimal leaf temperature (Matthews and Lawson, 2019; Stevens *et al.* 2021) and for photosynthesis and plant productivity (Moore *et al.*, 2021). Dynamic responses have been linked to both morphological and physiological variation in stomata (Drake *et al.*, 2013; Lawson and Blatt, 2014; Zhang *et al.*, 2019); however, few studies have explored the impact of changing climate conditions such as growth [CO_2] on morphophysiological characteristics. Consequently, natural variation in rapidity of stomatal conductance between cultivars and species, as well as the influence of changing climatic conditions on these traits, could provide currently unexploited targets for improving crop productivity in future climates (Lawson *et al.*, 2012; Faralli *et al.*, 2019; Faralli and Lawson, 2020).

Here we explored the impact of elevated CO_2 concentration (e[CO_2]) of 800 ppm, approximately double that of the current atmospheric [CO_2] (a[CO_2]), on the physiology and growth of 11 different wheat progenitor and elite cultivar accessions. Wheat (*Triticum aestivum* L.) is a principal global food grain source, grown on more land area than any other commercial crop. In addition, it is one of the largest traded primary crop commodities, along with maize and rice (FAO, 2014). Globally, wheat provides >20% of the calories consumed by the human population (Braun and Atlin, 2010; Lobell *et al.*, 2011). Modern wheat is a hexaploid species containing three sets of chromosomes (A, B, and D subgenomes). These subgenomes originated from three different diploid grass species and combined during two hybridization events (Kerber and Rowland, 1974; Faris, 2014; Marcussen *et al.*, 2014). Initially diploid wheat *Triticum urartu* (subgenome AA ancestor) hybridized with the B genome ancestor *Aegilops speltoides* ssp. *ligustica* (Huang *et al.*, 2002; Dvorak and Akhunov, 2005; Peng *et al.*, 2011) to produce wild emmer wheat *Triticum turgidum* ssp. *dicoccoides* (genome AABB). In the second event, *T. turgidum* ssp. *dicoccoides* hybridized with the wild goat grass *Aegilops tauschii* to produce the modern hexaploid *Triticum aestivum* ssp. *aestivum* (AABBDD; Huang *et al.*, 2002; Charmet, 2011; Faris, 2014). In this study, phenotypic variation in morphological traits including stomatal size and density, as well as physiological responses and, critically, the effect of growth [CO_2] on these traits, was assessed in six wheat relative (WR) accessions (including the species *Aegilops tauschii*, *T. turgidum* ssp. *dicoccoides*, and *T. turgidum* ssp. *dicoccon*) and five elite wheat *T. aestivum* cultivars (Claire, Rialto, Robigus, Soissons, and Xi19) to identify possible beneficial traits that could be exploited for future breeding.

Materials and methods

Plant growth conditions

Triticum and *Aegilops* species (listed in Table 1) were germinated in a greenhouse compartment (at BASF, Ghent, Belgium) with supplementary lighting (Master Greenpower CGT 400 W E40 HPS lights) to ensure a typical summer day length of 15.30 h. At 14 d post-emergence, plants were vernalized in a controlled environment (custom-made growth chamber, BASF, Ghent, Belgium) for 10 weeks at 4 °C, with 75 µmol m^{-2} s^{-1} PPFD, over a 10 h photoperiod using an in-house-produced 60/40 peat-based sowing and cutting soil (including NPK Compound Fertilizer 12-14-24 (0.8 kg m^{-3}). Plants were then transferred into 4 liter pots using a peat-based, boron-free potting soil [including NPK Compound Fertilizer 12-14-24 (2 kg m^{-3})] and grown in two separate growth environments, one at current (2018) atmospheric [CO_2] (408 ppm CO_2) and a second at an elevated [CO_2] of 800 ppm. Both growth chambers had a light intensity (at pot height) of 800 ± 20 µmol m^{-2} s^{-1} with a 2:1 high pressure sodium:metal halide lighting mix (Master Greenpower CGT 400 W E40 and Powerstar HQI-BT 400 W/D PRO 400 W Daylight E40, respectively) for a 15 h light/9 h dark photoperiod. With the exception of [CO_2], both growth environments were set to identical conditions: air temperature controlled to 20 °C and 18 °C (±1 °C) day and night, respectively, and relative humidity maintained at a constant 65%. Plants were well watered using a drip irrigation system to the roots. All wheat measurements were taken from the flag leaf, at Zadoks growth stage 49 (GS 49, first awns/scurs visible) to GS 59 (ear emergence complete) (Zadoks *et al.*, 1974). Six repetitions of each measurement were completed per accession unless stated below.

Leaf anatomical measurements

Measurements of stomatal density and size

Stomatal density (SD) was measured from impressions taken from both the adaxial (upper) and abaxial (lower) leaf surface using silicone impression material (Xantopren, Heraeus, Germany) following the methods of Weyers and Johansen (1985) using six leaves per species/cultivar, measured at the middle of the leaf lamina. SD, guard cell length (GCL; used as a proxy for stomatal size), and pore length (PL) were all measured via light microscopy (Olympus BX60, Essex, UK). Total magnification was 100-fold for SD measurements and 400-fold for GCL and PL measurements.

Anatomical maximum stomatal conductance (g_{smax}: mol m^{-2} s^{-1}) was calculated from the measurements of SD and stomatal dimensions (Equation 1) following the equations of Franks and Farquhar (2001):

$$(d \times \mathrm{SD} \times a_{\max}) / \{\nu \times [1 + (\pi/2) \times \sqrt{(a_{\max}/\pi)}]\} \quad (1)$$

Where d is the diffusivity of water in air (m^2 s^{-1}, at 22 °C), ν is the molar volume of air (m^3 mol^{-1}, at 22 °C), and pore depth (l; µm) was equal to guard cell width at the centre of the stoma represented as half the GCL. The mean maximum stomatal pore area (a_{max}; μm^2) was calculated assuming stomatal pores were elliptical with the major axis equal to pore length and the minor axis equal to half pore length (see McElwain *et al.*, 2015).

Leaf thickness

Leaf thickness (LT) measurements were taken using the MultispeQ v1.0 instrument (Michigan State University, MI, USA) (Kuhlgert *et al.*, 2016). The device was calibrated using 0.18 mm thick filter paper (Whatman 1001-110, Maidstone, Kent, UK). A mean leaf thickness was calculated from three repeat measurements per leaf from three separate leaves per species/cultivar.

Dry weight and leaf area

Leaf area was measured using a bench-top area meter (LI-3100C, Li-Cor, Lincoln, NE, USA) where the mean leaf area was calculated from three repeat measurements per leaf from three separate leaves per species/cultivar. Leaves were then placed in paper bags and dried at 60 °C to constant weight and measured using a four-digit balance (Kern, Northamptonshire, UK).

Leaf gas exchange

Stomatal conductance to water vapor (g_s) and the rate of photosynthetic CO_2 assimilation (A) were measured using a portable gas exchange system (Li-Cor 6400XT, Li-Cor) with an integrated light source (Li6400-40, Li-Cor), consisting of blue and red light-emitting diodes. Leaf temperature and VPD were controlled to 22 °C and 1 ± 0.2 kPa, respectively, throughout the measurements. Gas exchange measurements had a constant flow rate set at 300 µmol s^{-1}, with cuvette conditions maintained at a CO_2 concentration of 400 µmol mol^{-1} (for both plant growth CO_2 treatments). Gas exchange analysis was completed within the first 7 h of the photoperiod, to minimize any diurnal effects on stomatal opening and photosynthetic activation. All measurements were conducted on the mid-point of fully expanded flag leaves, before anthesis (GS 49–59) (Zadoks *et al.*, 1974). Intrinsic water use efficiency was calculated as $WUEi = A/g_s$. Between five and seven repetitions of each measurement were completed per accession for gas exchange data.

Table 1. Species investigated, including ploidy and common name

Species/cultivar abbreviation	Species	Common name	Ploidy
Claire	*Triticum aestivum*	Common or bread wheat	Hexaploid
Rialto	*Triticum aestivum*	Common or bread wheat	Hexaploid
Robigus	*Triticum aestivum*	Common or bread wheat	Hexaploid
Soissons	*Triticum aestivum*	Common or bread wheat	Hexaploid
Xi19	*Triticum aestivum*	Common or bread wheat	Hexaploid
TRI 11502	*Triticum dicoccoides*	Wild emmer	Tetraploid
TRI 3432	*Triticum dicoccon*	Emmer	Tetraploid
IG 48509	*Aegilops tauchii*	Goat grass or rough-spike hard grass	Diploid
IG48514	*Aegilops tauchii*	Goat grass or rough-spike hard grass	Diploid
KU2018	*Aegilops tauchii*	Goat grass or rough-spike hard grass	Diploid
KU 2036	*Aegilops tauchii*	Goat grass or rough-spike hard grass	Diploid

Species abbreviation is how the species is referred to in the text. All seeds were provided from the NIAB collection.

PPFD step measurements

To measure the response of A and g_s to a single step increase in PPFD, leaves were equilibrated at a PPFD of 100 µmol m^{-2} s^{-1} until both A and g_s were at steady state (defined as <2% change in rate over 5 min). Measurements were made at 30 s intervals, for 10 min at 100 µmol m^{-2} s^{-1}, after which PPFD was increased in a single step to 1000 µmol m^{-2} s^{-1} and recorded for a further 60 min. Leaf temperature (Ti), VPD, and [CO_2] were all maintained at 22 °C, 1 ± 0.2 kPa, and 400 µmol mol^{-1}, respectively, throughout the measurement. These data were used to model the response of A, g_s, and WUEi to changes in PPFD.

Intracellular CO_2 response curves (A/C_i)

A/C_i response curves [net CO_2 assimilation rate (A) to intercellular CO_2 concentration (C_i)] were measured at 1500 µmol m^{-2} s^{-1} PPFD. Photosynthesis was initially stabilized for a minimum of 15 min at 400 µmol mol^{-1}, then decreased and measured at 250, 150, 100, and 50 µmol mol^{-1} before returning to the initial value of 400 µmol mol^{-1}, and increased to 550, 700, 900, 1100, 1300, and 1500 µmol mol^{-1}. Photosynthesis was measured at each [CO_2] after ~3 min. Leaf temperature and VPD were controlled to 22 °C and 1 ± 0.5 kPa, respectively.

Modeling gas exchange parameters

The maximum velocity of Rubisco for carboxylation (V_{cmax}) and the maximum rate of electron transport demand for ribulose bisphosphate dehydrogenase (RuBP) regeneration (J_{max}) were calculated from the A/C_i response using equations from von Caemmerer and Farquhar (1981), as described by Sharkey *et al.* (2007) using the Rubisco kinetic constants for wheat (Carmo-Silva *et al.*, 2010). The response of g_s to the step change in PPFD was analyzed following the method described in McAusland *et al.* (2016). In summary, the optimum function in R (www.r-project.org; version 3.5.3), a model representing g_s as a function of time, was fitted on each observed response as shown in Equation 2:

$$g_s = (g_{smax} - r_0)\, e^{-e^{\left(\frac{\lambda - t}{k} + 1\right)}} + r_0 \quad (2)$$

The model uses a sigmoidal equation rather than an exponential slope, with an initial time lag (the time before g_s starts to increase, λ, min), a time constant (the time taken to reach 63% of the variation, k, min), an initial value (r_0, mol m^{-2} s^{-1}), and a steady-state target [the value when the plateau is reached (g_{smax}, mol m^{-2} s^{-1}]. The time was set to 0 when PPFD was increased from 100 µmol m^{-2} s^{-1} to 1000 µmol m^{-2} s^{-1} (Vialet-Chabrand *et al.*, 2013).

Statistical analysis

All statistical analyses were conducted using R software (www.r-project.org; version 3.5.3). For SD, GCL, and g_{smax}, a Shapiro–Wilk test was used to test for normality and a Levene's test of homogeneity was used to determine if samples had equal variance. A log transformation was applied when data were not normally distributed (P<0.05, Shapiro–Wilk test) to achieve normality and meet modeling assumptions of an ANOVA. Single factor differences were analyzed using t-tests with a Bonferroni–Hochberg end correction or a one-way ANOVA, as described in the figure legends. When more than one factor existed, a two-way ANOVA was applied with an interaction between the two factors, and, if a significant difference was found (P<0.05), a Tukey post-hoc test was performed.

Results

Stomatal anatomy

Stomatal anatomy including SD and GCL was measured in five elite *T. aestivum* cultivars (Claire, Rialto, Robigus, Soissons, and Xi19; all hexaploid) and six WRs (four diploid lines IG 48509, IG 48514, KU 2018, and KU 2036; and two tetraploid lines TRI 3432 and TRI 11502), grown at two [CO_2], atmospheric (a[CO_2]) at ~408 ppm and elevated (e[CO_2]) at ~800 ppm. Significant (P<0.05) variation in combined (adaxial+abaxial) leaf SD was found between species grown at a[CO_2] (Fig. 1A) with the hexaploid cultivars ranging from ~0 mm^2 to ~100 mm^2 and the wheat relatives showing a larger range of ~60 mm^2 to ~160 mm^2, with a +60% difference between the lowest and the highest mean SDs. When grown at e[CO_2] (Fig. 1B), less variation between and within species was observed. The majority of WRs showed a decrease in SD, with the exception of the *T. dicoccoides* accession TRI 11502 in which SD increased. No consistent pattern of change was observed for the elite hexaploid cultivars, with two cultivars showing no change in SD, while Rialto decreased, and Claire increased SD (P<0.05). SD was higher on the adaxial (upper) leaf surface (Fig. 1C) compared with the abaxial (lower) (Fig. 1E) surface (P<0.05) and SD on the adaxial surface was influenced to a greater extent by e[CO_2] (Fig. 1D) and accounted for a greater proportion of changes in total leaf SD compared with the abaxial surface, and this was particularly evident in the WRs. Overall, there was no relationship between SD in plants grown a[CO_2] and e[CO_2] (Supplementary Fig. S1A). However, those species showing a change in SD with e[CO_2] on the adaxial surface also had significantly altered SD on the abaxial surface, albeit of a smaller magnitude (Fig 1F). These data suggest that the majority of the combined (adaxial+abaxial) SD is determined by adaxial density (Fig. 1). Although there was no consistent species response of GCL to growth at e[CO_2] (Supplementary Fig. S2), a significant (P=0.0055) positive correlation was observed between GCL from plants grown at ambient and elevated [CO_2] (Supplementary Fig. S1B). The smallest GCL was observed for *Ae. tauschii* accession KU 2036 at ~29 µm at a[CO_2] and ~35 µm at e[CO_2], while the largest GCL was found on the bread wheat cultivars Xi19 at ~47 µm at a[CO_2] and Robigus at ~45 µm at e[CO_2]. When species were separated by ploidy, diploid species tended to respond to e[CO_2] by increasing GCL; however, this was not always significant (Supplementary Fig. S2). Tetraploids had a tendency to decrease in GCL, but no specific trends were observed for hexaploids. Unlike the case for SD, it appears that average leaf GCL was determined by both the adaxial and abaxial leaf surfaces, as similar responses to e[CO_2] were observed on both, and together reflected the observed differences in combined (adaxial+abaxial) leaf averages (Supplementary Fig. S2).

A negative correlation between SD and GCL was evident for wheat grown at ambient [CO_2] (P≤0.001; Fig. 2A), demonstrating a relationship between decreasing SD and

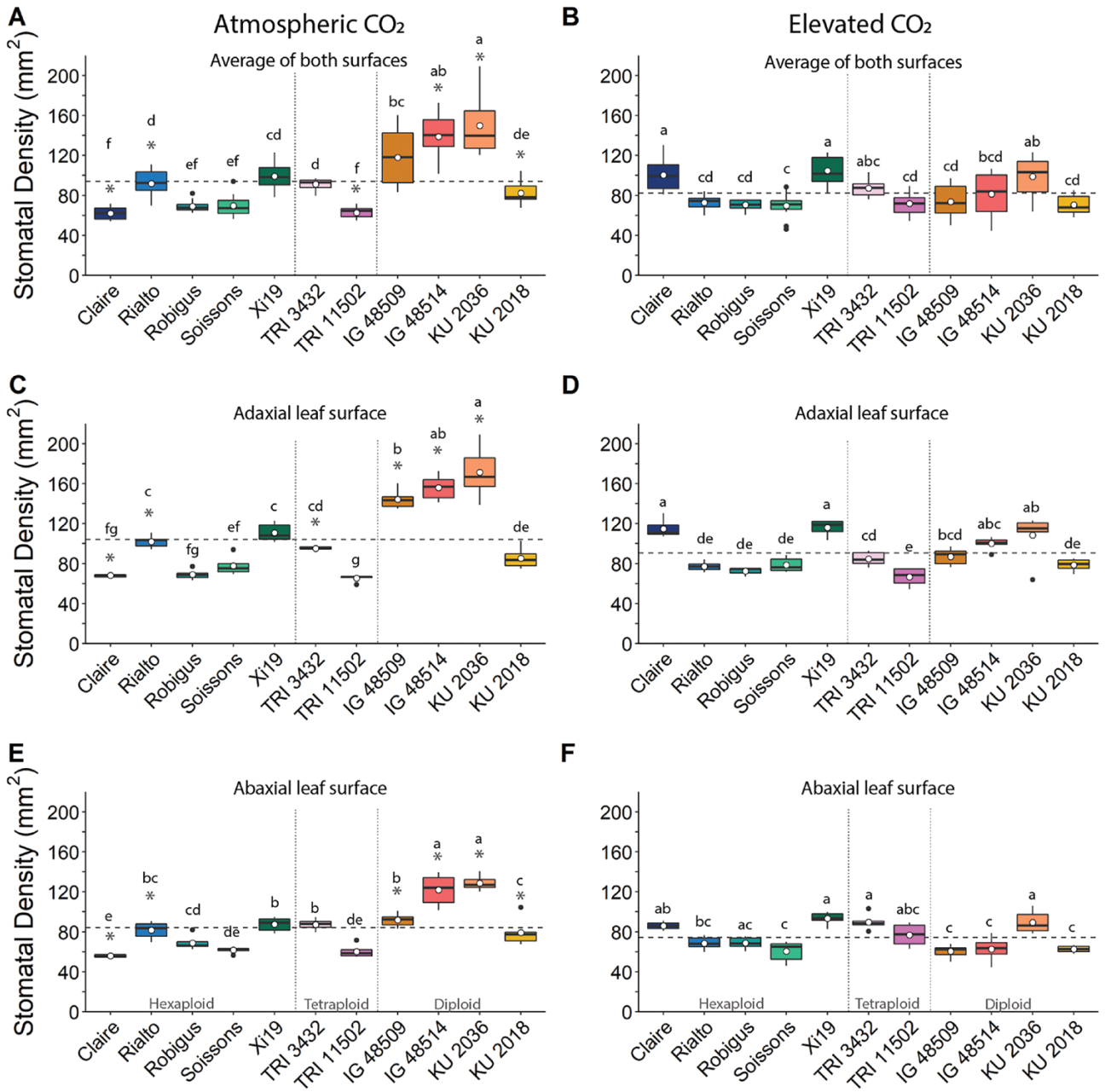

Fig. 1. Mean (white dot) and variation (box and whisker plots displaying distribution of biological replicates) of flag leaf stomatal density (mm^2), calculated from the average of both leaf surfaces (A and B), the adaxial leaf surface (C and D), and the abaxial leaf surface (E and F) for 11 wheat species grown at atmospheric CO2 (~408 ppm; A, C, and E) and elevated CO_2 (~800 ppm; B, D, and F). Different letters represent statistically significant differences (P<0.05) between species means using the results of a Tukey test following a two-way ANOVA. A dashed line represents mean stomatal density of all wheat lines for the specific CO_2 treatment and leaf surface. Dotted lines separate wheat by ploidy. To test the effect of growth at elevated [CO_2] on stomatal density, a *t*-test with a Bonferroni–Hochberg end correction (n=6) was used to compare stomatal density means of individual wheat lines, with gray asterisks indicating significant differences (P<0.05).

increasing stomatal size, driven mostly by the change in the four diploid accessions. *Aegilops tauschii* accession KU 2036 had the highest SD and smallest GCL, and the accession with the lowest SD mean (cv. Claire) had one of the largest GCLs. Although a similar trend of decreasing GCL with increasing SD was observed for the species and cultivars when grown under e[CO_2], this relationship was not significant (Fig. 2B). This is most likely to be attributable to the reduced range in SD under e[CO_2], particularly for the four *Ae. tauschii* accessions (Fig. 1B).

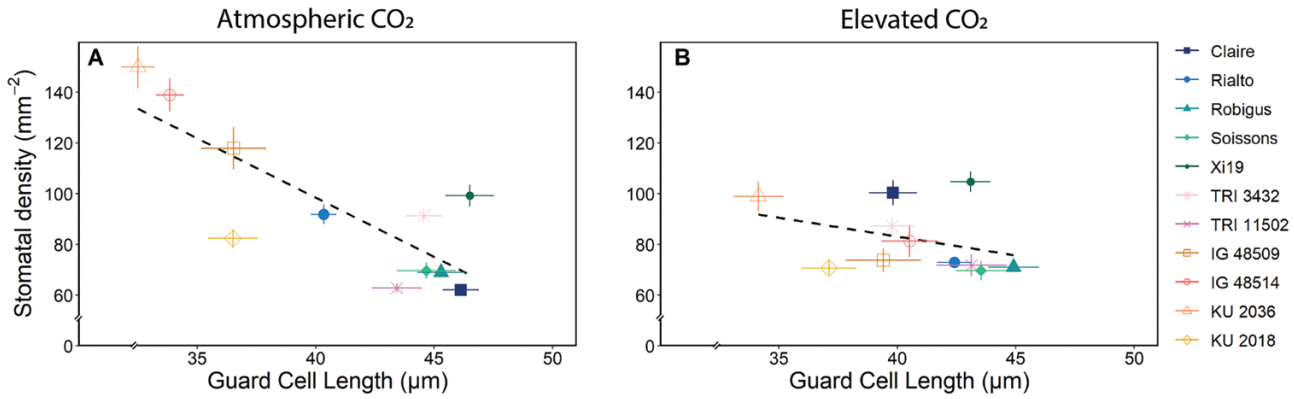

Fig. 2. Correlation between total stomatal density (mm^2) and total guard cell length (μm) for each species, calculated for the average of both leaf surfaces, for 11 wheat species grown at atmospheric CO_2 (~408 ppm; A) and elevated CO_2 (~800 ppm; B). The black dotted line represents the trend in the data between the two variables. Atmospheric CO_2 correlation= –0.552 (P=6.79e-12) and elevated CO_2 correlation=0.0625 (P=0.483) using a Pearson's correlation test. Error bars represent the SE (n=12).

Anatomical potential maximum rate of g_s

SD and measurements of stomatal size (GCL) were used to calculate the maximum anatomical stomatal conductance (g_{smax}), assuming fully open pores. At a[CO_2], a considerable range of g_{smax} values were determined between accessions (Fig. 3A), with cv. Soissons displaying the lowest and *Ae. tauschii* accession KU 2036 the highest values (an increase of ~41%, driven predominantly by the differences in SD; Fig. 1). Higher g_{smax} values were observed on the adaxial leaf surface irrespective of growth [CO_2] (Fig. 3C, D), with typical values >1.0 mol m^{-2} s^{-1}, whereas g_{smax} values on the abaxial surface (except e[CO_2]-grown Xi19) were <1.0 mol m^{-2} s^{-1} (Fig. 3E, F). There was considerable variation in the response of g_{smax} when grown under e[CO_2] compared with a[CO_2] (Fig. 3B). These differences appear to be driven mostly by the changes in SD (Fig. 1), but not exclusively as the CO_2 response patterns between SD (Fig. 1) and g_{smax} (Fig. 3) were not identical. Similar to the patterns described for SD, there was a tendency for reduction in g_{smax} with e[CO_2] driven mostly by adaxial g_{smax}. However, interestingly, not all of the changes in SD translated into changes in g_{smax}, strongly indicating a role for changes in GCL with e[CO_2] to compensate for changes in density, maintaining a similar g_{smax} (Lawson and Morison, 2004; Harrison *et al.*, 2020; Wall *et al.*, 2022); for example, the diploid and tetraploid species have similar g_{smax} to that of the hexaploid species even though SD is much higher in the diploid species.

Leaf gas exchange

Response of *gs* and *A* to a step change in PPFD

The effect of e[CO_2] on stomatal behavior/kinetics was assessed by measurements of g_s and A following a step increase in PPFD (Fig. 4). As expected, all species and cultivars exhibited an increase in g_s and A with increasing irradiance. In general, A rapidly increased compared with g_s when light was increased (Fig. 4A–D), and this resulted in the maximum WUEi value being reached within a few minutes of the change in PPFD (Fig. 4E, F). Further increases in g_s with time drove a continuous decrease in WUEi, and this trend continued after A had reached a maximum steady state. Considerable variation in A, g_s, and WUEi was observed in plants grown under both [CO_2] treatments, although the variation was more apparent in growth at e[CO_2], particularly for A and g_s (Fig. 4A–D).

The time constant to reach 63% of the final value for g_s (τ_{gs}) as an indicator of the rapidity (Fig. 5) was significantly greater (P<0.05) in the hexaploid wheat compared with other species, regardless of growth [CO_2] (Fig. 5A, B). Hexaploid lines averaged 20 min to reach maximum g_s while the other species averaged 10 min. In general, e[CO_2] increased the time constant (indicating slower stomatal responses) in most species with the exception of cv. Claire and *T. dicoccon* accession TRI 3432 which showed no significant differences, and *T. dicoccoides* accession TRI 11502 and cv. Xi19 which were significantly faster with e[CO_2] (Fig. 5B). Interestingly, there was a significant positive correlation (P<0.05) between τ_{gs} in plants grown at ambient [CO_2] and at e[CO_2], indicating that speed was inherent with limited influence of growth environment (Supplementary Fig. S3). However, the speed of the g_s response did not influence the overall final g_s (g_{sF}) achieved (Fig. 5C–F), with no correlation observed between the two. Growth at e[CO_2] did not influence g_{sF} values, with no differences observed between most accessions, with the exception of cv. Soissons and KU 2018 (Fig. 5C, D). On the other hand, the magnitude of change in g_s (Δg_s) decreased in almost all species and cultivars with growth at e[CO_2], with the exception of the hexaploid cv. Rialto and Robigus and the *Ae. tauschii* accession IG 48509, and this was related to the speed of response, with slow responding accessions (mostly the hexaploids) having a lower Δg_s compared with the fast responders in which Δg_s was greater (Fig. 5E), although this correlation was only significant (at P=0.0107) when plants were grown under

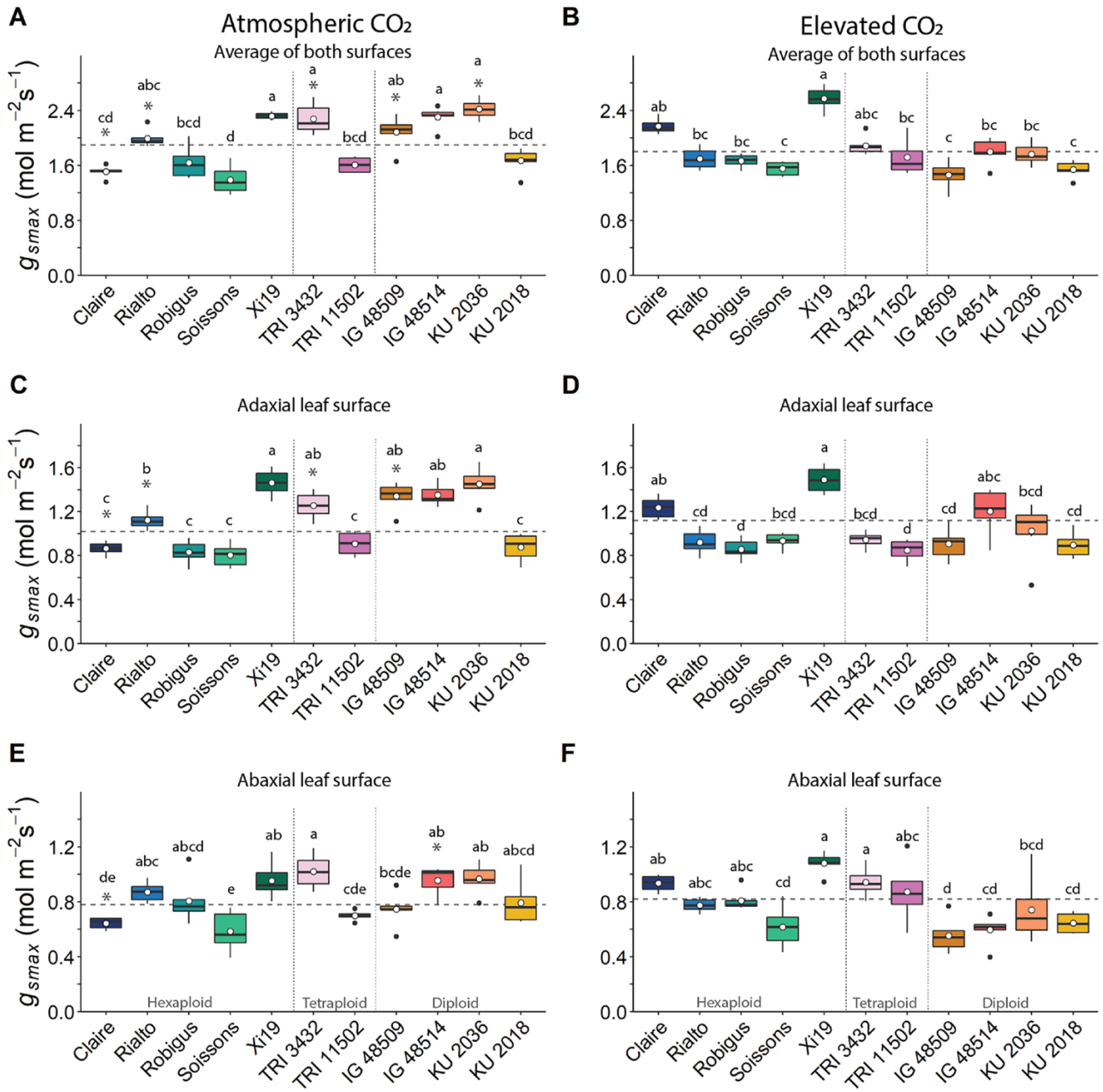

Fig. 3. Mean (white dot) and variation (box and whisker plots displaying distribution of biological replicates) of flag leaf g_{smax} (mol m^{-1} s^{-1}), calculated from the average of both leaf surfaces (A and B), the adaxial leaf surface (C and D), and the abaxial leaf surface (E and F) for 11 wheat species grown at atmospheric CO_2 (~408 ppm; A, C, and E) and elevated CO_2 (~800 ppm; B, D, and F). Different letters within each graph represent statistically significant differences (P<0.05) between means using the results of a Tukey test following a two-way ANOVA. The dashed line represents the mean g_{smax} of specific CO_2 treatment and leaf surface. Dotted lines separate wheat by ploidy. To test the effect of growth at elevated [CO_2] on g_{smax}, a t-test with a Bonferroni–Hochberg end correction (n=6) was used to compare individual wheat line means, with gray asterisks indicating significant differences (P<0.05).

e[CO_2] and not significant at ambient a[CO_2] (Supplementary Fig. S4A, B). The fact that there was no effect of e[CO_2] on g_{sF} indicates that minimum g_s must have been higher with growth at high [CO_2]. The more rapid g_s responses did not, however, impact on τ_A (Fig. 6), with no clear relationship between the two parameters. Δg_s was positively correlated with g_{sF} at both a[CO_2] and e[CO_2] (Supplementary Fig. S4C, D). Under both ambient and elevated growth [CO_2] conditions, the greater the g_{sF}, the higher the A_F achieved (Supplementary Fig. S4E, F), and under ambient but not elevated [CO_2] this was also correlated with a greater change in A (ΔA) (Supplementary Fig. S4G, H), suggesting diffusion constraints by g_s on the kinetic responses of A. The final value of A (A_F, Fig. 6) at 1000 µmol m^{-2} s^{-1} PPFD was similar across the different accessions, ~25 µmol m^{-2}

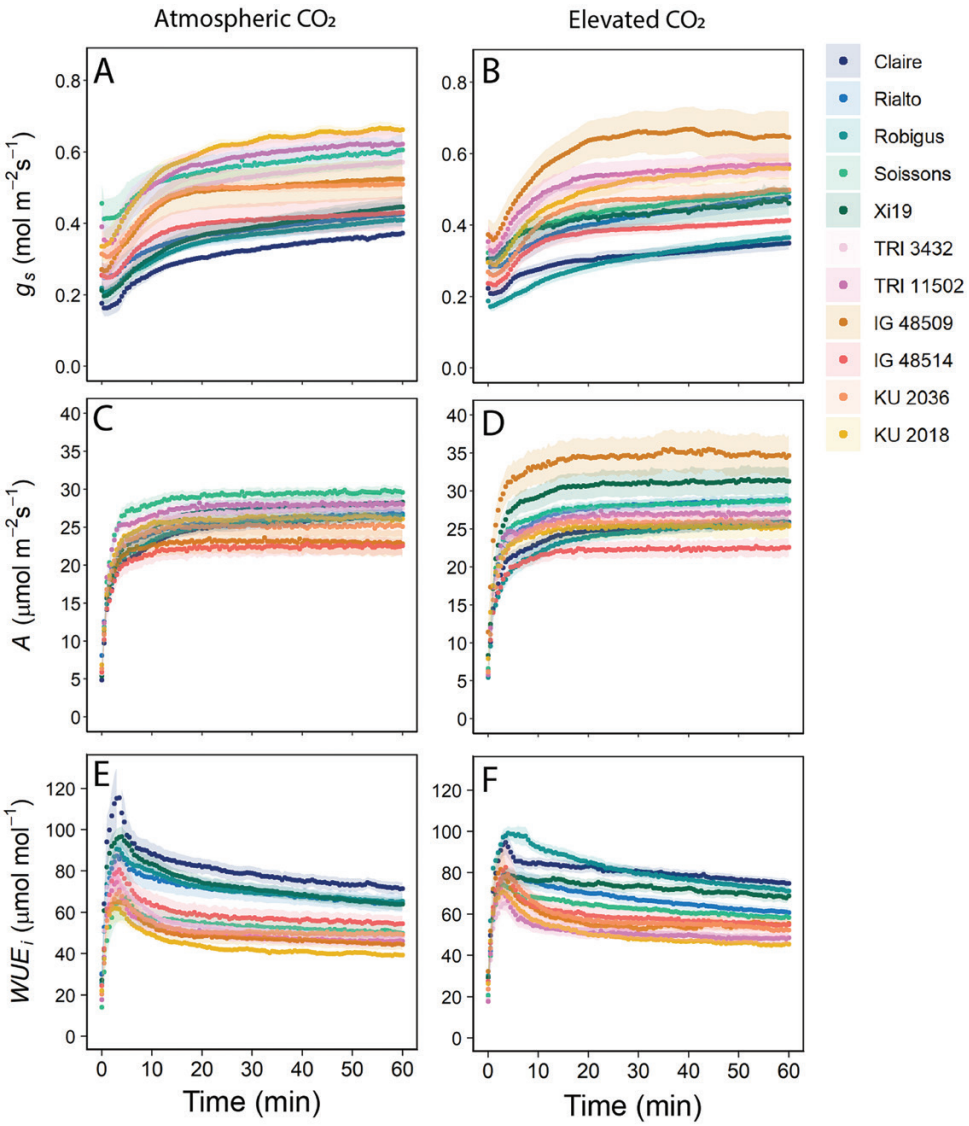

Fig. 4. Temporal response of stomatal conductance (g_s; A and B), net CO_2 assimilation (A; C and D), and intrinsic water use efficiency (WUEi; E and F), to a step increase in light intensity (from 100 µmol m^{-1} s^{-1} to 1000 µmol m^{-1} s^{-1} PPFD for 60 min) for 11 wheat species grown at atmospheric CO_2 (~408 ppm) and elevated CO_2 (~800 ppm). Gas exchange parameters (g_s and A) were recorded at 30 s intervals, and leaf temperature and VPD were maintained at 22 °C, and 1 ± 0.2 kPa, respectively. Error ribbons represent the mean ±SE (n=5–7).

s^{-1} for both CO_2 growth treatments, although values for two accessions were significantly (P<0.05) higher when grown at e[CO_2], hexaploid cv. Xi19, ~32 µmol m^{-2} s^{-1} and *Ae. tauschii* accession IG 48509, ~35 µmol m^{-2} s^{-1}, and, not unexpectedly, this was highly positively correlated with the ΔA (Supplementary Fig. S4I, J). The change in A (ΔA) was similar across the different species, showing a typical increase of 15 µmol m^{-2} s^{-1} with a few exceptions being higher at 20 µmol m^{-2} s^{-1} (Fig. 6E, F). However, there was no relationship between τ_A and these values in plants grown under e[CO_2] (Fig. 6), but the speed of the A response was negatively correlated with g_{sF}, suggesting possible differences in the induction of photosynthesis due to both stomatal and biochemical constraints (Supplementary Fig. S4K, L).

A/C_i *response analysis*

In order to assess changes to photosynthetic capacity, the response of assimilation rate (A) as a function of internal [CO_2] (C_i; Supplementary Fig. S5) was determined on the flag leaf on plants grown in the two [CO_2] environments. All accessions exhibited the expected increase in A with increased C_i before reaching a plateau. Accessions grown at ambient [CO_2] displayed significant variation in their responses (Supplementary Fig. S5A). In general, hexaploid accessions had the highest assimilation rates, and greater V_{cmax}, J_{max}, and A_{max} values at both ambient and e[CO_2] (Supplementary Fig. S6) whilst those of the tetraploid and diploid species were lower, indicating a reduced photosynthetic capacity. Growth under e[CO_2] had no significant influence on photosynthetic capacity, in any of the species.

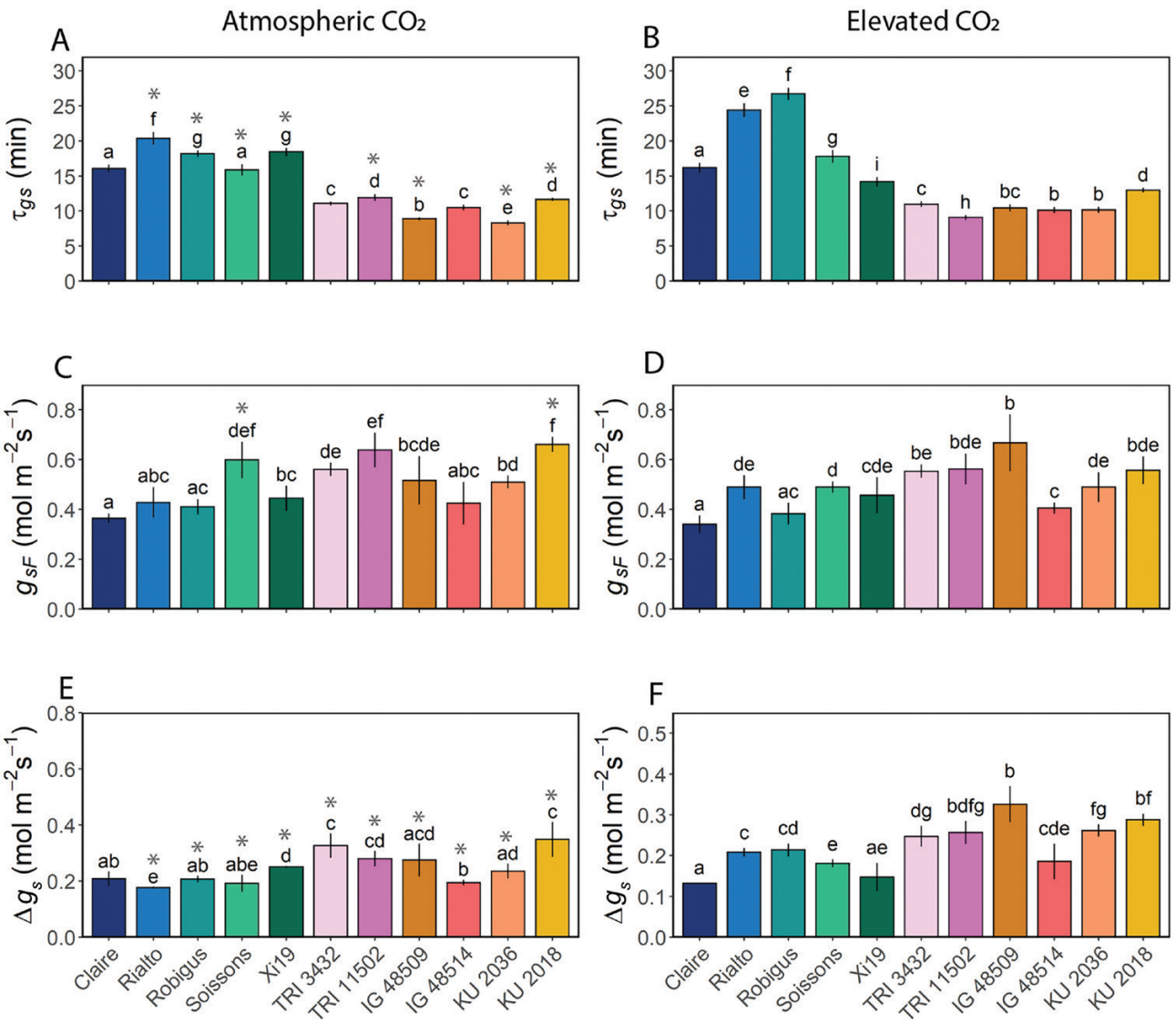

Fig. 5. Time constant for stomatal opening [τ_{gs} (min); A and B], final stomatal conductance value [g_{sF} (mol m^{-2} s^{-1}); B and D] after a step increase in light intensity from 100 μmol m^{-2} s^{-1} to 1000 μmol m^{-2} s^{-1} PPFD, and the difference in g_s [Δ_{gs} (mol m^{-2} s^{-1})] between 100 μmol m^{-2} s^{-1} and 1000 μmol m^{-2} s^{-1} PPFD (E and F). The 11 wheat species were grown at both at atmospheric [CO_2] (~408 ppm; A, C, and E) and elevated [CO_2] (~800 ppm; B, D, and F). Error bars represent 95% confidence intervals using the results of a Tukey test following a two-way ANOVA. To test the effect of growth at elevated [CO_2], a *t*-test with a Bonferroni–Hochberg end correction (n=5–7) was used to compare individual wheat line means, with gray asterisks indicating significant differences (P<0.05).

Plant growth

Multiple leaf growth parameters were measured including flag leaf area (LA; Supplementary Fig. S7), DW (Supplementary Fig. S8), and leaf thickness (LT; Supplementary Fig. S8). In general, all hexaploid wheat accessions had a greater LA (Supplementary Fig. S7) than other species, except for the tetraploid *T. dicoccon* accession TRI 3432 when grown at a[CO_2]. A similar trend followed for e[CO_2]-grown wheat, although there was less variation between species. No significant differences were observed between accessions from the same species from a[CO_2] to e[CO_2] except for *Ae. tauschii* accession IG 48509 in which LA increased. DW (Supplementary Fig. S8) followed the same trends as LA. In general, there was a trend for hexaploid and tetraploid species having thicker leaves than the diploid species at both CO_2 growth treatments (Supplementary Fig. S9), the exception being cv. Soissons in which LT was reduced at e[CO_2]. These data suggest that the diploid species had smaller thinner leaves compared with the hexaploid wheat species.

Discussion

The global human population is expected to reach >9.5 billion by 2050, putting increasing pressure on breeders and crop scientists to improve yields to ensure sufficient food (Asseng *et al.*,

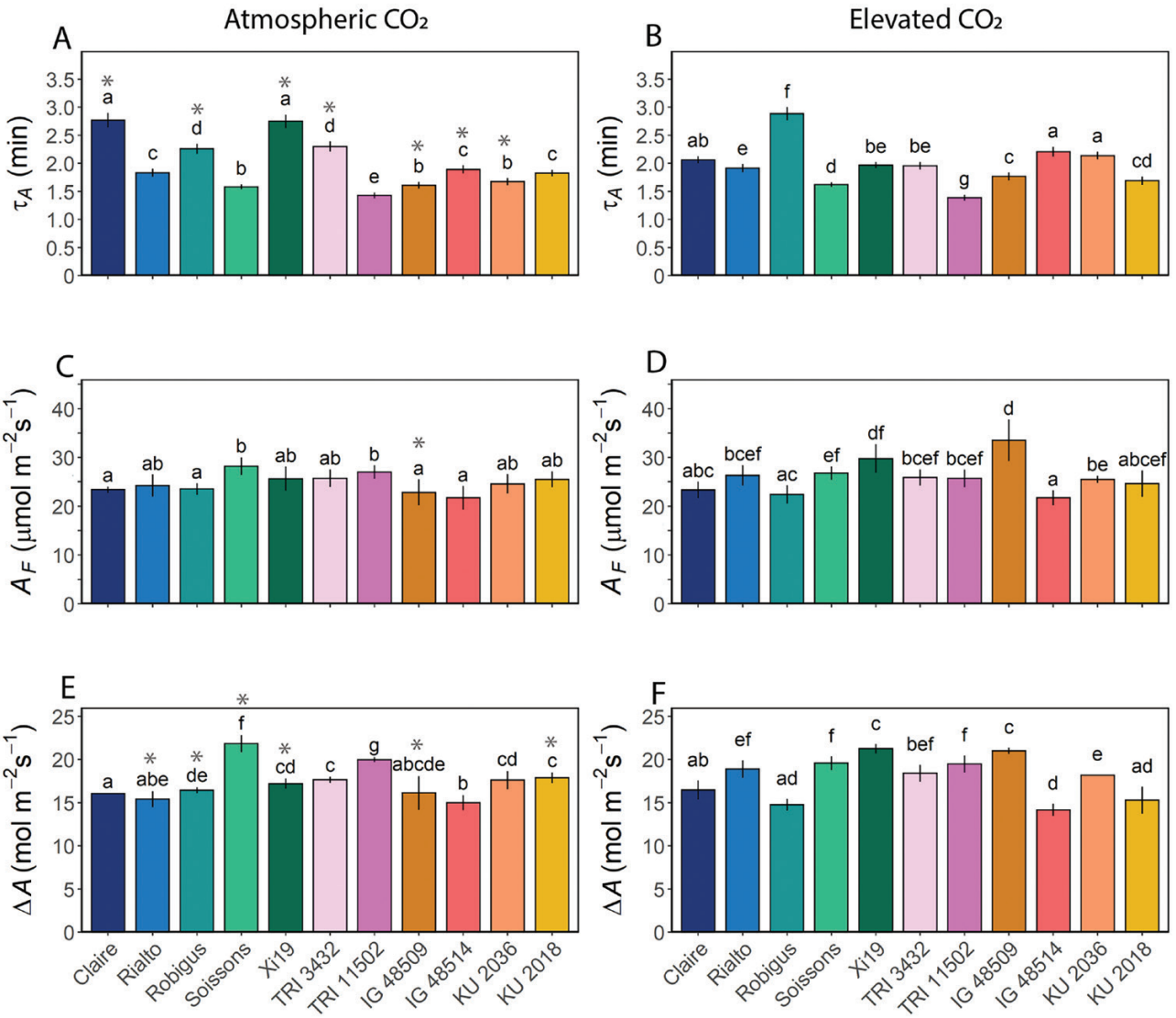

Fig. 6. Time constant for light-saturated carbon assimilation [τ_A (min); A and B), final light-saturated carbon assimilation rate [A_F (μmol m^{-2} s^{-1}); B and D] after a step increase in light intensity from 100 μmol m^{-2} s^{-1} to 1000 μmol m^{-2} s^{-1} PPFD, and the difference in A [ΔA (μmol m^{-2} s^{-1})] between 100 μmol m^{-2} s^{-1} and 1000 μmol m^{-2} s^{-1} PPFD (E and F). The 11 wheat species were grown at both at atmospheric [CO_2] (~408 ppm; A, C, and E) and elevated [CO_2] (~800 ppm; B, D, and F). Error bars represent 95% confidence intervals using the results of a Tukey test following a two-way ANOVA. To test the effect of growth at elevated [CO_2], a *t*-test with a Bonferroni–Hochberg end correction (n=5–7) was used to compare individual wheat line means, with gray asterisks indicating significant differences (P<0.05).

2020). However, with the continued increases in global [CO_2], along with predicted changes to climate, it is vital that crop improvement programs consider the impact of these changes on crop performance and identify valuable physiological resilience traits (and the underlying genetics) that maintain productivity in a diverse range of environmental conditions. Genetic engineering approaches have demonstrated that enhancing photosynthetic capacity and stomatal behavior can successfully deliver crops with greater yield and resource use efficiency (Ruiz-Vera *et al.*, 2017; López-Calcagno *et al.*, 2020; De Souza *et al.*, 2022). However, another powerful approach is exploiting natural variation in various physiological traits including photosynthesis (Driever *et al.*, 2014; Carmo-Silva *et al.*, 2017; Faralli and Lawson, 2019) and stomatal dynamics (Faralli *et al.*, 2019, 2022; Sakoda *et al.*, 2022). Exploiting variation in current elite bread wheat germplasm (e.g. Driever *et al.*, 2014; Faralli *et al.*, 2019) as well as crop relatives (McAusland *et al.*, 2020; Sharwood *et al.*, 2022) offers significant potential to identify novel allelic variation (Sakoda *et al.*, 2022; Sharwood *et al.*, 2022; Yin *et al.*, 2022). Here we have explored the impact of growth [CO_2] on variation in photosynthesis, stomatal anatomy, and stomatal kinetics in several elite wheat cultivars and their tetraploid and diploid relatives.

It is well documented that significant variation in stomatal anatomy exists between and within species, spatially within

leaves (Ticha, 1982; Smith *et al.*, 1989; Willmer and Fricker, 1996; Weyers and Lawson, 1997; Weyers *et al.*, 1997) and on different leaf surfaces (Wall *et al.*, 2022), all of which are influenced by the growth environment (Poole *et al.*, 1996; Croxdale, 2000; Lawson *et al.*, 2002). Stomatal density is one of the most plastic traits and is affected by a great number of environmental parameters (Matthews and Lawson, 2019; Stevens *et al.*, 2021). Increasing growth [CO_2] most commonly decreases SD in the majority of plant species investigated (Woodward, 1987), but not all (Lodge *et al.*, 2001), and the degree of change is not the same even within cultivars of the same species (Dusenge *et al.*, 2019). Not unexpectedly, in this study we observed significant variation across and between species and cultivars. The highest SDs were observed in the tetraploid relatives, with some individuals having double that of some elite varieties. A possible explanation for the high SD in the WRs is the smaller leaf area in these species (Supplementary Fig. S7). Therefore, expansion or differentiation of the epidermal cells in the elite cultivars would reduce SD (Lawson *et al.*, 2002). Interestingly, growth at e[CO_2] generally reduced SD in diploid species, but not in the elite cultivars (except Rialto), and therefore no relationship between SD in plants grown under the two [CO_2] was observed (Supplementary Fig. S1). Furthermore, variation within and between cultivars was generally reduced at e[CO_2], although the underlying cause of the reduced variation is currently unknown. However, as these plants were grown in controlled environments, and the only changing variable was [CO_2] (with all other parameters kept constant), it is possible that plants grown at a[CO_2] were subjected to greater variation in [CO_2] (due to photosynthetic draw down), and that the plants were more sensitive and responsive to this variation. For example, the a[CO_2] growth chambers ware maintained at 400 ppm; however, photosynthetic CO_2 fixation would result in short-term dynamic draw down of [CO_2] to ~320 ppm, whilst the same draw down in e[CO_2] would result in variation only between 700 ppm and 800 ppm, and plants would be less sensitive to these changes (Franks *et al.*, 2012) as these levels will saturate photosynthesis (Supplementary Figs S2, S3).

The SD variation and response to [CO_2] were mainly the result of anatomical changes on the adaxial leaf surface, suggesting two important points. Firstly, the receptors or signaling pathways responsible for detecting and responding to growth at e[CO_2] which drive changes in stomatal patterning are complex and either they reside separately on the two surfaces (and are not mesophyll driven) or there is limited surface to surface communication. Secondly, stomata on the adaxial surface play a more prominent role in gaseous exchange than those on the abaxial surface. This agrees with the recent work by Wall *et al.* (2022) who demonstrated that adaxial stomata make the greatest contribution to leaf gas exchange in amphistomatous bread wheat. Tsutsumi *et al.* (2014) reported that elevated [CO_2] decreased leaf size in rice, and this was accompanied by a decrease in epidermal cell numbers on the adaxial surface, but a reduction in cell size on the abaxial surface, thus providing a possible explanation for the differences observed between surfaces in different cultivars. GCL (as an indicator of stomatal size) was generally lower in the WRs compared with the elite cultivars, and together with SD was used to determine the maximum potential g_s (g_{smax}) for the accessions investigated. As above, the variation in g_{smax} was driven mostly by SD (and at the leaf level due to differences on the adaxial surface), but not entirely, with GCL clearly having a secondary role, as has previously been shown (Lawson and Morison, 2004). These findings indicate that there are some compensatory processes between SD and GCL (or size) to maintain a level of g_{smax} across species (Lawson and Morison, 2004; Bussis *et al.*, 2006; McElwain *et al.*, 2016). The strong negative correlation observed between SD and stomatal size in plants grown at ambient [CO_2] agrees with several reports that have shown that lowered SD results in increased size (Franks and Farquhar, 2007). What is particularly interesting is that this size–density relationship was lost in plants grown at e[CO_2], due in part to the decrease in SD variation with growth at e[CO_2], and the fact that no relationship between SD at the two growth [CO_2] were observed; however, GCL was positively correlated between plants grown in the two environments. The anatomical constraints of g_{smax} can translate into species-specific differences in operational or functional g_s (McElwain *et al.*, 2016), often with implications for carbon gain and water use efficiency—particularly in dynamic environments (Vialet-Chabrand *et al.*, 2016; Lawson and Vialet Chabrand, 2019). Dynamic stomatal responses and the speeds of stomatal responses to changing environmental cues have recently received considerable attention for optimizing A relative to water loss and WUEi (Farquhar and Sharkey, 1982; Mansfield *et al.*, 1990; Lawson *et al.*, 2010; Buckley and Mott, 2013; Lawson and Blatt, 2014; Buckley, 2017; Vialet-Chabrand *et al.*, 2017; Matthews *et al.*, 2018; Papanatsiou *et al.*, 2019; Yamori *et al.*, 2020). Stomatal conductance, although closely correlated with A, is an order of magnitude slower to respond to these changes than photosynthetic responses and can therefore lead to a disconnect between A and g_s, as slow stomatal opening can limit CO_2 uptake whilst slow closure can erode water use efficiency (Drake *et al.*, 2013; Lawson and Vialet-Chabrand, 2019; Vialet-Chabrand and Lawson, 2019). Exploiting variation in kinetic stomatal responses has been proposed as a possible route to increase the speed of stomatal responses to be more in tune with photosynthetic demands for CO_2 (Lawson *et al.*, 2018). We know that stomatal kinetics depend on species (McAusland *et al.*, 2016), cultivar (McAusland *et al.*, 2020; Stevens *et al.*, 2021), environmental conditions (Ainsworth and Long, 2005, 2021; De Souza *et al.*, 2020), and time of day (Matthews *et al.*, 2017). Here the kinetic responses of g_s to increasing PPFD were up to 50% slower in the elite cultivars compared with the diploid and tetraploid WRs, and growth at e[CO_2] decreased the speed even further. This agrees with previous reports that g_s responses are slower in species with a lower density of larger guard cells (e.g. Elliott-Kingston

et al., 2016) as we have observed here in the WRs, and growth under elevated [CO_2] could amplify this, dampening the g_s response (Knapp *et al.*, 1994). Surprisingly, these differences did not directly translate into differences in final g_s values at high PPFD, most probably due to greater variation in τ_{gs} than g_{sF}. However, slow g_s responses did result in a lower Δg_s under e[CO_2], implying that stomatal speed influences overall g_s behavior at elevated but not a[CO_2]. This is most likely to be due to a greater variation in g_s in plants grown under e[CO_2]. Δg_s was positively correlated with g_{sF} (Supplementary Fig. S4), further supporting the idea that stomatal kinetics influence overall g_s behavior and final values achieved. Such a relationship has previously been shown for tobacco, with the greater the change the higher the g_s value achieved (von Caemmerer *et al.*, 2004). Together, these findings indicate that both anatomical and biochemical/physiological components determine the speed of g_s responses (Lawson and Blatt, 2014) and that both the rapidity in stomatal responses and the magnitude of change influence g_s values. Growth under e[CO_2] reduced the magnitude of change in g_s following the step increase in PPFD; however, it is clear that this was driven by differences in minimum g_s and not the maximum achieved (g_{sF}). This could be due to differences in SD with growth under e[CO_2] or that guard cell sensitivity to [CO_2] was reduced under these conditions, ultimately increasing g_s at low light (Hetherington and Woodward, 2003; Chater *et al.*, 2015). The final g_s values (g_{sF}) positively correlated with A_F at ambient and elevated [CO_2] (Supplementary Fig. S4), clearly demonstrating a diffusional constraint on photosynthetic induction rates, and highlights the importance of stomatal behavior in carbon assimilation (Lawson *et al.*, 2012; De Souza *et al.*, 2020; Long *et al.*, 2022). g_{sF} also positively correlated with ΔA, providing further support for a diffusional constraint on A. The fact that a similar relationship was not observed in plants grown at e[CO_2] is most probably due to g_{sF} not being influenced by growth at e[CO_2] and therefore decreased g_s control on CO_2 diffusion and A. The negatively correlation between g_{sF} and τ_A (at both growth [CO_2]) illustrates the importance of g_s in photosynthetic induction (Lawson *et al.*, 2010; Long *et al.*, 2022). Furthermore, the tight correlation between ΔA and A_F (Supplementary Fig. S4) suggests that photosynthetic capacity at low PPFD was less variable than at high PPFD, and the final A reached depends on the magnitude and kinetic changes in A, that are driven by both stomatal and biochemical traits (Lawson *et al.*, 2012).

The kinetic responses revealed more variation between accessions in both A and g_s at e[CO_2] compared with ambient; however, the two compensated for changes in one relative to the other to maintain a similar WUEi to plants grown in ambient conditions. This demonstrates the importance of measuring both physiological components that make up WUEi as well as the attributing anatomical features (Lawson *et al.*, 2010). The strong correlation between the speed of g_s at ambient [CO_2] and e[CO_2] indicates that the rapidity of g_s depends on stomatal anatomy and biochemistry, and not only differences in photosynthetic biochemistry. This is also supported by the lack of any influence that growth [CO_2] had on V_{cmax}, A_{max}, and J_{max} (Supplementary Fig. S6). Therefore, stomatal speed is an inherent trait within these species and cultivars, supporting the notion that such a phenotype could be a key trait which could be incorporated for future breeding programmes.

In conclusion, this study has demonstrated that there is significant variation between species and cultivars in stomatal anatomy and function as well as photosynthetic capacity, and that growth at e[CO_2] does not necessarily impact on all of them, or in the same way. Current hexaploid bread wheat has a number of desirable traits, such as larger leaves and higher photosynthetic capacity, lower SD with a small Δg_s (and therefore potential water saving capacity) compared with their WRs. Furthermore, SD in these species was not influenced by growth at e[CO_2]. It is possible that these traits have been unintentionally selected for during the breeding process. However, the WRs have much faster stomatal kinetics compared with modern wheat species, and although here this did not directly translate into improved A (as in previous studies) it was directly related to g_{sF} which correlated significantly with A_{max} (Supplementary Fig. S4), suggesting some reduced stomatal diffusional constraints on A in cultivars with greater Δg_s. Such phenotyping traits could also be beneficial for increased WUEi as well as maintaining optimal leaf temperatures, highlighting the potential to exploit natural variation in different species, WRs, and elite crop varieties to develop idiotypes to maintain productivity in future climates.

Supplementary data

The following supplementary data are available at *JXB* online.

Fig. S1. Correlation between SD and GCL of 11 wheat species grown at a[CO_2] and e[CO_2].

Fig. S2. Variation of flag leaf guard cell length of both abaxial and adaxial leaf surfaces for 11 wheat species grown at a[CO_2] and e[CO_2].

Fig. S3. Correlations between the time constant for stomatal opening of wheat species grown at a[CO_2] and e[CO_2].

Fig. S4. Correlation between kinetic parameters for 11 wheat species grown at a[CO_2] and e[CO_2].

Fig. S5. The response of net CO_2 assimilation to intercellular [CO_2] under saturating PPFD for 11 wheat species grown at a[CO_2] and e[CO_2].

Fig. S6. Photosynthetic capacity including the maximum RuBP-saturated rate of carboxylation, the maximum RuBP-saturated rate of carboxylation, and the light- and CO_2-saturated rate of photosynthesis for 11 wheat species grown at a[CO_2] and e[CO_2].

Fig. S7. Variation of flag leaf area for 11 wheat species grown at a[CO_2] and e[CO_2].

Fig. S8. Variation of flag leaf dry weight for 11 wheat species grown at a[CO_2] and e[CO_2].

Fig. S9. Variation of flag leaf thickness for 11 wheat species grown at a[CO_2] and e[CO_2].

Acknowledgements

We would like to acknowledge the team of from BASF, Belgium for assistance and support with growing plants and data collection.

Author contributions

SW and TL: designing the experiments and writing the manuscript; SW: performing all experiments and data acquisition; SW, SVC, and TL: data analysis; SVC: modeling and analyzing the induction data. All authors contributed to editing the manuscript.

Conflict of interest

No conflict of interest declared.

Funding

SW was supported by a Biotechnology and Biological Sciences Research Council (BBSRC) industrial studentship (1775930) awarded to BASF (JVR), Essex (TL), and NAIB (JC). SV-C was supported by the Global Challenges Research Fund as part of TIGR2ESS: Transforming India's Green Revolution by Research and Empowerment for Sustainable Food Supplies (BB/P027970/1) awarded to TL. TL also acknowledges funding support through the BBSRC IWYP Programme (BB/S005080/1).

Data availability

The data that support the findings of this study are openly available from this link: http://researchdata.essex.ac.uk/165/

References

Acevedo-Siaca LG, Dionora J, Laza R, Paul Quick W, Long SP. 2021. Dynamics of photosynthetic induction and relaxation within the canopy of rice and two wild relatives. Food and Energy Security **10**, e286.

Ainsworth EA, Long SP. 2005. What have we learned from 15 years of free-air CO_2 enrichment (FACE)? A meta-analytic review of the responses of photosynthesis, canopy properties and plant production to rising CO_2. New Phytologist **165**, 351–371. doi:10.1111/j.1469-8137.2004.01224.x.

Ainsworth EA, Long SP. 2021. 30 years of free-air carbon dioxide enrichment (FACE): what have we learned about future crop productivity and its potential for adaptation? Global Change Biology **27**, 27–49. doi:10.1111/gcb.15375.

Asseng S, Guarin JR, Raman M, Monje O, Kiss G, Despommier DD, Meggers FM, Gauthier PPG. 2020. Wheat yield potential in controlled-environment vertical farms. Proceedings of the National Academy of Sciences, USA **117**, 19131–19135.

Braun HJ, Atlin GPT. 2010. Multi-location testing as a tool to identify plant response to global climate change. In: Reynolds MP, ed. Climate change and crop production. Wallingford, UK: CABI Publishing, 115–138.

Buckley TN. 2017. Modeling stomatal conductance. Plant Physiology **174**, 572–582.

Buckley TN, Mott KA. 2013. Modelling stomatal conductance in response to environmental factors. Plant, Cell & Environment **36**, 1691–1699.

Bussis D, von Groll U, Fisahn J, Altmann T. 2006. Stomatal aperture can compensate altered stomatal density in *Arabidopsis thaliana* at growth light conditions. Functional Plant Biology **33**, 1037–1043.

Carmo-Silva E, Andralojc PJ, Scales JC, Driever SM, Mead A, Lawson T, Raines CA, Parry MAJ. 2017. Phenotyping of field-grown wheat in the UK highlights contribution of light response of photosynthesis and flag leaf longevity to grain yield. Journal of Experimental Botany **68**, 3473–3486. doi:10.1093/jxb/erx169.

Carmo-Silva AE, Keys AJ, Andralojc PJ, Powers SJ, Arrabaça, MCParry, MAJ. 2010. Rubisco activities, properties, and regulation in three different C4 grasses under drought. Journal of Experimental Botany **61**, 2355–2366. doi:10.1093/JXB/ERQ071.

Charmet G. 2011. Wheat domestication: lessons for the future. Comptes Rendus Biologies **334**, 212–220.

Chater C, Peng K, Movahedi M, *et al*. 2015. Elevated CO_2-induced responses in stomata require ABA and ABA signaling. Current Biology **25**, 2709–2716. doi:10.1016/j.cub.2015.09.013.

Croxdale JL. 2000. Stomatal patterning in angiosperms. American Journal of Botany **87**, 1069–1080.

De Souza AP, Burgess SJ, Doran L, Hansen J, Manukyan L, Maryn N, Gotarkar D, Leonelli L, Niyogi KK, Long SP. 2022. Soybean photosynthesis and crop yield are improved by accelerating recovery from photoprotection. Science **377**, 851–854.

De Souza AP, Wang Y, Orr DJ, Carmo-Silva E, Long SP. 2020. Photosynthesis across African cassava germplasm is limited by Rubisco and mesophyll conductance at steady state, but by stomatal conductance in fluctuating light. New Phytologist **225**, 2498–2512. doi:10.1111/NPH.16142.

Doheny-Adams T, Hunt L, Franks PJ, Beerling DJ, Gray JE. 2012. Genetic manipulation of stomatal density influences stomatal size, plant growth and tolerance to restricted water supply across a growth carbon dioxide gradient. Philosophical Transactions of the Royal Society B: Biological Sciences **367**, 547–555.

Dow GJ, Berry JA, Bergmann DC. 2014. The physiological importance of developmental mechanisms that enforce proper stomatal spacing in *Arabidopsis thaliana*. New Phytologist **201**, 1205–1217. doi:10.1111/nph.12586.

Drake PL, Froend RH, Franks PJ. 2013. Smaller, faster stomata: scaling of stomatal size, rate of response, and stomatal conductance. Journal of Experimental Botany **64**, 495–505.

Driever SM, Lawson T, Andralojc PJ, Raines CA, Parry MAJJ. 2014. Natural variation in photosynthetic capacity, growth, and yield in 64 field-grown wheat genotypes. Journal of Experimental Botany **65**, 4959–4973. doi:10.1093/jxb/eru253.

Dusenge ME, Duarte AG, Way DA. 2019. Plant carbon metabolism and climate change: elevated CO_2 and temperature impacts on photosynthesis, photorespiration and respiration. New Phytologist **221**, 32–49. doi:10.1111/NPH.15283.

Dvorak J, Akhunov ED. 2005. Tempos of gene locus deletions and duplications and their relationship to recombination rate during diploid and polyploid evolution in the *Aegilops–Triticum* alliance. Genetics **171**, 323–332.

Elliott-Kingston C, Haworth M, Yearsley JM, Batke SP, Lawson T, McElwain JC. 2016. Does size matter? Atmospheric CO_2 may be a stronger driver of stomatal closing rate than stomatal size in taxa that diversified under low CO_2. Frontiers in Plant Science **7**, 1253.

FAO. 2014. Wheat—the largest primary commodity. Rome: Food and Agriculture Organization.

Faralli M, Bontempo L, Bianchedi PL, Moser C, Bertamini M, Lawson T, Camin F, Stefanini M, Varotto C. 2022. Natural variation in stomatal dynamics drives divergence in heat stress tolerance and contributes to the seasonal intrinsic water-use efficiency in *Vitis vinifera* (subsp. *sativa* and *sylvestris*). Journal of Experimental Botany **73**, 617–648.

Faralli M, Cockram J, Ober E, Wall S, Galle A, Van Rie J, Raines C, Lawson C. 2019. Genotypic, developmental and environmental effects on

the rapidity of gs in wheat: impacts on carbon gain and water-use efficiency. Frontiers in Plant Science **10**, 492.

Faralli M, Lawson T. 2020. Natural genetic variation in photosynthesis: an untapped resource to increase crop yield potential? The Plant Journal **101**, 518–528.

Faris JD. 2014. Wheat domestication: key to agricultural revolutions past and future. In: Tuberosa R, Graner A, Frison E, eds. Genomics of plant genetic resources., pp. 439–464. Springer, Dordrecht, the Netherlands.

Farquhar GD, Sharkey TD. 1982. Stomatal conductance and photosynthesis. Annual Review of Plant Physiology **33**, 317–345.

Franks PJ, Farquhar GD. 2001. The effect of exogenous abscisic acid on stomatal development, stomatal mechanics, and leaf gas exchange in *Tradescantia virginiana*. Plant Physiology **125**, 935–942.

Franks P, Farqhuar GD. 2007. The mechanical diversity of stomata and its significance in gas-exchange control. Plant Physiology **143**, 78–87.

Franks PJ, Freckleton RP, Beaulieu JM, Leitch IJ, Beerling DJ. 2012. Megacycles of atmospheric carbon dioxide concentration correlate with fossil plant genome size. Philosophical Transactions of the Royal Society B: Biological Sciences **367**, 556–564.

Harrison EL, Arce Cubas L, Gray JE, Hepworth C. 2020. The influence of stomatal morphology and distribution on photosynthetic gas exchange. The Plant Journal **101**, 768–779. doi:10.1111/tpj.14560.

Hetherington AM, Woodward FI. 2003. The role of stomata in sensing and driving environmental change. Nature **424**, 901–908.

Huang S, Sirikhachornkit A, Su X, Faris J, Gill B, Haselkorn R, Gornicki P. 2002. Genes encoding plastid acetyl-CoA carboxylase and 3-phosphoglycerate kinase of the *Triticum/Aegilops* complex and the evolutionary history of polyploid wheat. Proceedings of the National Academy of Sciences, USA **99**, 8133–8138.

IPCC. 2021. Climate Change 2021: the physical science basis. Contribution of Working Group I to the Sixth Assessment Report of the Intergovernmental Panel on Climate Change. Cambridge, UK: Cambridge University Press.

Kerber ER, Rowland GG. 1974. Origin of the free threshing character in hexaploid wheat. Canadian Journal of Genetics and Cytology **16**, 145–154.

Knapp AK, Fahnestock JT, Owensby CE. 1994. Elevated atmospheric CO_2 alters stomatal responses to variable sunlight in a C_4 grass. Plant, Cell & Environment **17**, 189–195.

Kuhlgert S, Austic G, Zegarac R, *et al*. 2016. MultispeQ Beta: a tool for large-scale plant phenotyping connected to the open photosynQ network. Royal Society Open Science **3**, 160592.

Lawson T, Blatt M. 2014. Stomatal size, speed and responsiveness impact on photosynthesis and water use efficiency. Plant Physiology **164**, 1556–1570. doi:10.1104/pp.114.237107.

Lawson T, Craigon J, Black CR, Colls JJ, Tullock AM, Landon G. 2001. Effects of elevated carbon dioxide and ozone on the growth and yield of potatoes (*Solanum tuberosum*) grown in open-top chambers. Environmental Pollution **111**, 479–491. doi:10.1016/S0269-7491(00)00080-4.

Lawson T, Craigon J, Black CR, Colls JJ, Landon G, Weyers JDB. 2002. Impact of elevated CO_2 and O_3 on gas exchange parameters and epidermal characteristics in potato (*Solanum tuberosum* L.). Journal of Experimental Botany **53**, 737–746. doi:10.1016/s0269-7491(00)00080-4.

Lawson T, Kramer DM, Raines CA. 2012. Improving yield by exploiting mechanisms underlying natural variation of photosynthesis. Current Opinions in Plant Biotechnology **23**, 215–220. doi:10.1016/j.copbio.2011.12.012.

Lawson T, Morison JI. 2004. Stomatal function and physiology. In: Hemsley AR, Poole I, eds. The evolution of plant physiology: from whole plants to ecosystem. Cambridge, UK: Elsevier Academic Press, 217–242.

Lawson T, Terashima I, Fujita T, Wang Y. 2018. Co-ordination between photosynthesis and stomatal behaviour. In: Sharkey TD, Govindje, eds. The leaf: a platform for performing photosynthesis and feeding the plant. Cham: Springer, 141–161.

Lawson T, Vialet-Chabrand S. 2019. Speedy stomata, photosynthesis and plant water use efficiency. New Phytologist **221**, 93–98. doi:10.1111/nph.15330.

Lawson T, von Caemmerer S, Baroli I. 2010. Photosynthesis and stomatal behaviour. Progress in Botany **72**. doi:10.1007/978-3-642-13145-5_11.

Lawson T, Weyers JDB, A'brook R. 1998. The nature of heterogeneity in stomatal behaviour of *Phaseolus vulgaris* L. primary leaves. Journal of Experimental Botany **49**, 1387–1395. doi:10.1093/jxb/49.325.1387.

Leakey ADB, Ainsworth EA, Bernacchi CJ, Rogers A, Long SP, Ort DR. 2009. Elevated CO_2 effects on plant carbon, nitrogen, and water relations: six important lessons from FACE. Journal of Experimental Botany **60**, 2859–2876. doi:10.1093/jxb/erp096.

Lobell DB, Schlenker W, Costa-Roberts J. 2011. Climate trends and global crop production since 1980. Science **333**, 616–620.

Lodge RJ, Dijkstra P, Drake BG, Morison JIL. 2001. Stomatal acclimation to increased CO_2 concentration in a Florida scrub oak species *Quercus myrtifolia* Willd. Plant, Cell & Environment **24**, 77–88. doi:10.1046/j.1365-3040.2001.00659.x.

Long SP, Taylor SH, Burgess SJ, Carmo-Silva E, Lawson T, De Souza A, Leonelli L, Wang Y. 2022. Into the shadows and back into sunlight: photosynthesis in fluctuating light. Annual Review of Plant Biology **73**, 617–648.

López-Calcagno PE, Brown KL, Simkin AJ, Fisk SJ, Vialet-Chabrand S, Lawson T, Raines CA. 2020. Stimulating photosynthetic processes increases productivity and water-use efficiency in the field. Nature Plants **6**, 1054–1063. doi:10.1038/s41477-020-0740-1.

Mansfield TA, Hetherington AM, Atkinson CJ. 1990. Some current aspects of stomatal physiology. Annual Review of Plant Physiology and Plant Molecular Biology **41**, 55–75.

Marcussen T, Sandve SR, Heier L, *et al*. 2014. Ancient hybridizations among the ancestral genomes of bread wheat. Science **345**, 1250092.

Matthews JA, Lawson T. 2019. Climate change and stomatal physiology. Annual Plant Reviews **2**, doi:10.1002/9781119312994.apr0667

Matthews JA, Vialet-Chabrand SR, Lawson T. 2017. Diurnal variation in gas exchange: the balance between carbon fixation and water loss. Plant Physiology **174**, 614–623. doi:10.1104/pp.17.00152.

Matthews JS, Vialet-Chabrand SR, Lawson T. 2018. Acclimation to fluctuating light impacts the rapidity and diurnal rhythm of stomatal conductance. Plant Physiology **176**, 1939–1951.

McAusland L, Vialet-Chabrand S, Davey P, Baker NR, Brendel O, Lawson T. 2016. Effects of kinetics of light-induced stomatal responses on photosynthesis and water-use efficiency. New Phytologist **211**, 1209–1220.

McAusland L, Vialet-Chabrand S, Jauregui I, *et al*. 2020. Variation in key leaf photosynthetic traits across wheat wild relatives is accession-dependent not species-dependent. New Phytologist **228**, 1767–1780.

McElwain JC, Montañez IP, White JD, Wilson JP. 2016. Was atmospheric CO_2 capped at 1000 ppm over the past 300 million years? Palaeogeography, Palaeoclimatology, Palaeoecology **441**, 653–658.

McElwain JC, Yiotis C, Lawson T. 2015. Using modern plant trait relationships between observed and theoretical maximum stomatal conductance and vein density to examine patterns of plant macroevolution. New Phytologist **209**, 94–103. doi:10.1111/nph.13579.

Moore CA, Meacham-Hensold K, Lemonnier P, Slattery RA, Benjamin C, Bernacchi C, Lawson T, Cavanagh AP. 2021. The effect of increasing temperature on crop photosynthesis: from enzymes to ecosystems. Journal of Experimental Botany **72**, 2822–2844.

Morison JIL, Baker N, Mullineaux P, Davies W. 2008. Improving water use in crop production. Philosophical Transactions of the Royal Society B: Biological Sciences **363**, 639–658.

Murray RR, Emblow MSM, Hetherington AM, Foster GD. 2016. Plant virus infections control stomatal development. Scientific Reports **6**, 34507. doi:10.1038/srep34507.

NOAA. 2022. Climate change: atmospheric carbon dioxide. Earth System Research Laboratory. Available at: www.esrl.noaa.gov. Accessed: 20/07/2022.

Papanatsiou M, Petersen J, Henderson L, Wang Y, Christie JM, Blatt MR. 2019. Optogenetic manipulation of stomatal kinetics improves carbon assimilation, water use, and growth. Science **363**, 1456–1459.

Peng JH, Dongfa S, Nevo SE, Peng JH, Sun D, Nevo E. 2011. Domestication evolution, genetics and genomics in wheat. Molecular Breeding **28**, 281–301.

Peterson KM, Rychel AL, Torii KU. 2010. Out of the mouths of plants: the molecular basis of the evolution and diversity of stomatal development. The Plant Cell **22**, 296–306.

Pignon CP, Leakey ADB, Long SP, Kromdijk J. 2021. Drivers of natural variation in water-use efficiency under fluctuating light are promising targets for improvement in Sorghum. Frontiers in Plant Science **12**, 627432.

Poole I, Weyers JDB, Lawson T, Raven JA. 1996. Variations in stomatal density and index: implications for palaeoclimatic reconstructions. Plant, Cell & Environment **19**, 705–712.

Qu M, Essemine J, Xu J, *et al*. 2020. Alterations in stomatal response to fluctuating light increase biomass and yield of rice under drought conditions. The Plant Journal **104**, 1334–1347.

Qu M, Hamdani S, Li W, *et al*. 2016. Rapid stomatal response to fluctuating light: an under-explored mechanism to improve drought tolerance in rice. Functional Plant Biology **43**, 727.

Raven JA. 1977. The evolution of vascular land plants in relation to supracellular transport processes. Advances in Botanical Research **5**, 153–219.

Raven JA. 2002. Selection pressures on stomatal evolution. New Phytologist **153**, 371–386.

Rogers A, Allen DJ, Davey PA, *et al*. 2004. Leaf photosynthesis and carbohydrate dynamics of soybeans grown throughout their life-cycle under free-air carbon dioxide enrichment. Plant, Cell & Environment **27**, 449–458. doi:10.1111/J.1365-3040.2004.01163.X.

Ruiz-Vera UM, De Souza AP, Long SP, Ort DR. 2017. The role of sink strength and nitrogen availability in the downregulation of photosynthetic capacity in field grown *Nicotiana tabacum* L. at elevated CO_2 concentration. Frontiers in Plant Science **8**, 998. doi:10.3389/FPLS.2017.00998/BIBTEX.

Sakoda K, Adachi S, Yamori W, Tanaka Y. 2022. Towards improved dynamic photosynthesis in C_3 crops by utilizing natural genetic variation. Journal of Experimental Botany **73**, 3109–3121. doi:10.1093/jxb/erac100.

Sakoda K, Yamori W, Shimada T, Sugano SS, Hara-Nishimura I, Tanaka Y. 2020. Higher stomatal density improves photosynthetic induction and biomass production in Arabidopsis under fluctuating light. Frontiers in Plant Science **11**, 589603.

Schlüter U, Muschak M, Berger D, Altmann T. 2003. Photosynthetic performance of an Arabidopsis mutant with elevated stomatal density (sdd1-1) under different light regimes. Journal of Experimental Botany **54**, 867–874.

Sharkey DT, Bernacchi CI, Farquhar GD, Singsaas EL. 2007. Fitting photosynthetic carbon dioxide response curves for C_3 leaves. Plant, Cell & Environment **30**, 1035–1040.

Sharwood RE, Quick WP, Sargent D, Estavillo GM, Silva-Perez V, Furbank RT. 2022. Mining for allelic gold: finding genetic variation in photosynthetic traits in crops and wild relatives. Journal of Experimental Botany **73**, 3085–3108. doi:10.1093/jxb/erac081.

Smith S, Weyers JDB, Berry WG. 1989. Variation in stomatal characteristics over the lower surface of *Commelina communis* leaves. Plant, Cell & Environment **12**, 653–659.

Sreeharsha RV, Sekhar KM, Reddy AR. 2015 Delayed flowering is associated with lack of photosynthetic acclimation in Pigeon pea (*Cajanus cajan* L) grown under elevated CO_2. Plant Science **231**, 82–93.

Stevens J, Faralli M, Wall S, Stamford JD, Lawson T. 2021. Stomatal responses to climate change. In: Becklin K, Ward K, Way DA, eds. Photosynthesis, respiration and climate change. Cham: Springer, 17–47.

StockwellC,GeigesA,RamalopeD,GiddenM,HareB,deVillafrancaCasa MJ, Moisio M, Hans F, Fekete H. 2021. Glasgow's 2030 credibility gap: net zero'slipservicetoclimateaction.https://climateactiontracker.org/publications/glasgows-2030-credibility-gap-net-zeros-lip-service-to-climate-action/

Takahashi S, Monda K, Negi J, Konishi F, Ishikawa S, Hashimoto-Sugimoto M, Goto N, Iba K. 2015. Natural variation in stomatal responses to environmental changes among *Arabidopsis thaliana* ecotypes. PLoS One **10**, e0117449. doi:10.1371/journal.pone.0117449.

Tanaka Y, Sugano SS, Shimada T, Hara-Nishimura I. 2013. Enhancement of leaf photosynthetic capacity through increased stomatal density in Arabidopsis. New Phytologist **198**, 757–764.

Tans P, Keeling R. 2016. Trends in atmospheric carbon dioxide. NOAA. Available online at: http://www.esrl.noaa.gov/gmd/ccgg/trends. Accessed: 20/ July 2022.

Ticha I. 1982. Photosynthetic characteristics during ontogenesis of leaves. 7. Stomata density and sizes. Photosynthetica **16**, 375–471.

Tsutsumi K, Konno M, Miyazawa SI, Miyao M. 2014. Sites of action of elevated CO_2 on leaf development in rice: discrimination between the effects of elevated CO_2 and nitrogen deficiency. Plant and Cell Physiology **55**, 258–268. doi:10.1093/jxb/erac447.

Vialet-Chabrand S, Dreyer E, Brendel O. 2013. Performance of a new dynamic model for predicting diurnal time courses of stomatal conductance at the leaf level. Plant, Cell & Environment **36**, 1529–1546.

Vialet-Chabrand S, Lawson T. 2019. Dynamic leaf energy balance: deriving stomatal conductance from thermal imaging in a dynamic environment. Journal of Experimental Botany **70**, 2839–2855.

Vialet-Chabrand S, Lawson T. 2020. Thermography methods to assess stomatal behaviour in a dynamic environment. Journal of Experimental Botany **71**, 2329–2338.

Vialet-Chabrand S, Matthews JSA, Brendel O, Blatt M, Wang Y, Hills A, Griffiths H, Rogers S, Lawson T. 2016. Modelling water use efficiency in a dynamic environment: an example using *Arabidopsis thaliana*. Plant Science **251**, 65–74. doi:10.1016/j.plantsci.2016.06.016.

Vialet-Chabrand SR, Matthews JSA, McAusland L, Blatt M, Griffiths H, Lawson T. 2017. Temporal dynamics of stomatal behaviour: modelling, and implications for photosynthesis and water use. Plant Physiology **174**, 603–613. doi:10.1104/pp.17.00125

von Caemmerer S, Farquhar GD. 1981. Some relationships between the biochemistry of photosynthesis and the gas exchange of leaves. Planta **153**, 376–387.

von Caemmerer S, Lawson T, Oxborough K, Baker NR, Andrews TJ, Raines CA. 2004. Stomatal conductance does not correlate with photosynthetic capacity in transgenic tobacco with reduced amounts of Rubisco. Journal of Experimental Botany **55**, 1157–1166.

Wall S, Vialet-Chabrand S, Davey P, Van Rie J, Galle A, Cockram J, Lawson T. 2022. Stomata on the abaxial and adaxial leaf surface contribute differently to leaf gas exchange and photosynthesis in wheat. New Phytologist **235**, 1743–1756.

Weyers JDB, Johansen LG. 1985. Accurate estimation of stomatal aperture from silicone rubber impressions. New Phytologist **101**, 109–115.

Weyers JDB, Lawson T. 1997. Heterogeneity in stomatal characteristics. Advances in Botanical Research **26**, 317–352.

Weyers JDB, Lawson T, Peng ZY. 1997. Variation in stomatal characteristics at the whole-leaf level. In: Van Gardingen PR, Foody GM, Curran PJ, eds. Scaling-up from cell to landscape. Cambridge, UK: Cambridge University Press, 129–149.

Willmer C, Fricker M. 1996. Stomata. Dordrecht: Springer Netherlands.

Woodward FI. 1987. Stomatal numbers are sensitive to increases in CO_2 from pre-industrial levels. Nature **327**, 617–618.

World Meteorological Organization. 2022. State of the global climate 2021. https://library.wmo.int/index.php?lvl=notice_displayandid=21880#.Yw9oPnbMKUl

Yamori W, Kusumi K, Iba K, Terashima I. 2020. Increased stomatal conductance induces rapid changes to photosynthetic rate in response to naturally fluctuating light conditions in rice. Plant, Cell & Environment **43**, 1230–1240.

Yin X, Gu J, Dingkuhn M, Struik PC. 2022. A model-guided holistic review of exploiting natural variation of photosynthesis traits in crop improvement. Journal of Experimental Botany **73**, 3173–3188. doi:10.1093/jxb/erac109.

Zadoks JC, Chang TT, Konzak CF. 1974. A decimal code for the growth stages of cereals. Weed Research **14**, 415–421.

Zhang Q, Peng S, Li Y. 2019. Increase rate of light-induced stomatal conductance is related to stomatal size in the genus *Oryza*. Journal of Experimental Botany **70**, 5259–5269.